S. C. Ceuca and *D. Laurinavicius*

Experimental and numerical investigations on the direct contact condensation phenomenon in horizontal flow channels and its implications in nuclear safety

The complex direct contact condensation phenomenon is investigated in horizontal flow channels both experimentally and numerically with special emphasis on its implications on safety assessment studies. Under certain conditions direct contact condensation can act as the driving force for the water hammer phenomenon with potentially local devastating results, thus posing a threat to the integrity of the affected NPP components. New experimental results of in-depth analysis of the direct contact condensation phenomena obtained in Kaunas at the Lithuanian Energy Institute will be presented. The German system code ATHLET employing for the calculation of the heat transfer coefficient a mechanistic model accounting for two different eddy length scales, combined with the interfacial area transport equation will be assessed against condensation induced water hammer experimental data from the integral thermal-hydraulic experimental facility PMK-2, located at the KFKI Atomic Energy Research Institute in Budapest Hungary.

Experimentelle und numerische Untersuchungen des Phänomens Kontaktkondensation in horizontalen Strömungskanälen und sein Einfluss auf Reaktorsicherheitsanalysen. *Das komplexe Phänomen der Kontaktkondensation in horizontalen Strömungskanälen wurde sowohl experimentell als auch numerisch in Hinblick auf dessen Folgen für Reaktorsicherheitsanalysen untersucht. Unter bestimmten Bedingungen kann die Kontaktkondensation als treibende Kraft für Druckstöße wirken und somit lokal potentiell zerstörerische Kräfte freisetzen, wodurch die Integrität von Kraftwerkskomponenten gefährdet ist. In diesem Beitrag werden zum einen Ergebnisse von hochaufgelösten Messungen der Kontaktkondensation an der Versuchsanlage des Lithuanian Energy Instituts vorgestellt und zum anderen Ergebnisse von Simulationsrechnungen mit dem Systemcode ATHLET zu Kondensationsschlägen. In letzteren werden zum einen Rechnungen mit einem mechanistischen Modell zur Berechnung des Wärmeübergangskoeffizient basierend auf zwei Wirbelgrößen und zum anderen Rechnungen mit einer Transportgleichung für die Zwischenphasenfläche durchgeführt. Die Ergebnisse werden mit Messdaten zu Kondensationsschlagversuchen der Integralversuchsanlage PMK-2 des KFKI Atomic Energy Research Instituts in Budapest verglichen.*

1 Introduction

The understanding and the study of multiphase flow is of great interest in the safety driven nuclear industry. Interfacial phase change is a common phenomenon encountered in many components of a NPP facility. A correct understanding and modeling of the physics of two-phase-flow plays a crucial role during the design phase of new equipment, its efficient operation, as well as during the safety assessment studies. The realistic modelling of interfacial heat and mass transfer process such as the Direct Contact Condensation (DCC) phenomenon is a key goal for best-estimate simulations of Condensation Induced Water Hammer (CIWH) events. During these scenarios DCC acts as the driving force of the pressure surge event. The prompt and potentially violent CIWH event generates additional local mechanical loads, for example on the pipe structure. If this additional load is not considered during the design phase it can eventually result in mechanical components failure, thus jeopardizing the system integrity. Experimental and numerical investigations on the CIWH phenomenon was triggered by the U.S. Nuclear Regulatory Commission in the 1970's after the incident occurring at the nuclear power plant Indian Point No. 2, [1]. On the other hand the CIWH phenomena, if triggered in a controlled way, can be exploited to suddenly release a high amount of energy from a purely hydraulic capacitor-like device, [2]. This energy can be used for instance to power a cyclically operated device, envisioning a number of beneficial uses such as: to transfer liquid against the force of gravity, [3]. For the investigation of the beneficial effect of steam implosion, condensation and heat removal from the interface to the water bulk, an experimental rectangular channel was developed at the Lithuanian Energy Institute (LEI) in Kaunas. The facility is equipped with various instrumentation devices such as an infrared camera able to record the water temperature profiles with a high resolution in the case of a stratified co-current two-phase flow, thus offering valuable measurement data for the validation of CFD codes.

Modern system analysis codes are extensively used for deterministic safety assessment studies or designing industrial facilities with potentially exhibiting fluid-dynamic transients, such as water hammer events. Modern system codes are capable in modelling complex flow interactions in relatively large piping networks and system components by making use of sophisticated numerical and physical models to describe single- and multi-phase flows as realistically as possible. The system code ATHLET (Analysis of THermal-hydraulics of LEaks

and Transients) developed by Gesellschaft für Anlagen- und Reaktorsicherheit (GRS) is used for these applications. Assuming that DCC occurs on a saturated interface, two of the key variables which have to be modelled within the code, to correctly capture the phase change, are the Interfacial Area Concentration (IAC) and the Heat Transfer Coefficient (HTC). The latest release version ATHLET 3.1A includes a very new DCC model. This model extends the applicability to simulate the phenomenon of CIWH employing mechanistic models for the calculation of the IAC and the HTC. In this paper verification and validations analyses by comparing ATHLET calculation results with experimental data of the PMK-2 facility are presented. There, a nodalization study was included, too.

2 Theoretical background of direct contact condensation phenomenon

The DCC describes a phase change that takes place at the two-phase interface of direct contact between liquid and vapor. The two-phase interface is assumed to be at saturation condition through the entire process, whereas the liquid and/or the steam can be away from saturation, but the interface is not considered to add any resistance to the heat and mass transfer between the phases.

A scenario in which DCC plays an important role within a nuclear power plant is during a postulated LOCA, especially during the re-flooding stage as sub-cooled water is injected by the Emergency Core Cooling System (ECCS) into the primary side pipes and it flows counter-currently to the steam exiting the reactor core. Accurate safety related studies of the re-flooding stage of a LOCA with computer tools, require models that can predict condensation rates as correctly as possible, particularly at locations close to the injection point of the ECCS or in areas of high flow turbulence which, together with a high sub-cooling of the water in contact with the saturated or superheated steam can lead to sudden flow regime changes and very fast condensation of the steam. The analysis of the local effects during the re-flooding stage of a LOCA is very complex due to the highly dynamic character of the two-phase flow. The calculation of DCC must consider several key parameters that describe the macroscopic phase change phenomena, such as the local heat transfer coefficient (HTC), the area of contact between both phases (interfacial area), and the sub-cooling of the liquid phase. The first two parameters have to be correctly predicted using special models in the computer simulations, while the last one is a direct consequence of the solved conservation equations with a strong feedback from the first two parameters.

A reliable prediction of the transient flow patterns is required, in addition to the correct modeling of the heat and mass transfer processes over the wide range of two-phase flow regimes. Flow patterns that can occur in horizontal or nearly horizontal flow channels can be grouped based on local parameters such as the phase specific superficial velocities and local void fraction. These flow patterns span for a horizontal two-phase flow from stratified to slug flow with entrainment of the disperse phase, which can be both steam bubbles and water droplets depending on the two-phase flow configuration and void fraction.

For the theoretical and fundamental investigation of the DCC phenomenon various experimental facilities have been designed and constructed. One of the modern one, equipped with state of the art sensors is located at the Lithuanian Energy Institute in Kaunas.

In some particular cases DCC can lead to a special case of water hammer events, as steam condenses on the liquid water surface of a two phase flow creating a local depressurization since the specific volume of steam is much larger than that of liquid. This event is illustrated in Fig. 1 based on a horizontal two-phase flow between steam (represented with the white color) and sub-cooled water (represented with the grey color). This depressurization results in water being accelerated while filling the volume left empty by steam condensation, second illustration from the top in Fig. 1. A CIWH can occur when the steam pocket in the condensing region collapses and the liquid fronts rushing to fill them collide, third illustration from the top in Fig. 1. Experimental investigations on the CIWH phenomenon have been recently done in Germany within the Condensation Induced WAter Hammer (CIWA) research alliance, [4] and [5].

3 Modelling approach of the direct contact condensation phenomenon

In order to model the DCC phenomenon specific closure laws have to be employed. The closure laws for the modelling of interfacial friction and of the interfacial mass and energy transfer depend on the actual flow structure. In previous ATHLET versions, flow regimes were determined using different functions in dependence of local void fractions and phase velocities at each time step, while assuming fully developed flows. Neither scaling effects nor the temporal and spatial evolution of flow patterns were taken into account adequately.

Significant modelling improvement is expected by the simulation of the time evolution of two-phase flow regimes, [6]. One first step towards this was the implementation of an additional field equation in ATHLET, based on the interfacial area concentration transport equation together with the use of a mechanistic heat transfer model. The IAC and the HTC are two key parameters for the determination of the interfacial heat and mass exchange terms, acting as source or sink terms in the considered two-phase conservation equations. The interfacial area concentration corresponds to the ratio of interfacial area available in any computational cell to the cell's total volume. The additional transport equation has the typical form for any scalar while special source and sink terms have to be defined that account for the various mechanisms of interfacial area increase or decrease. The original form of the

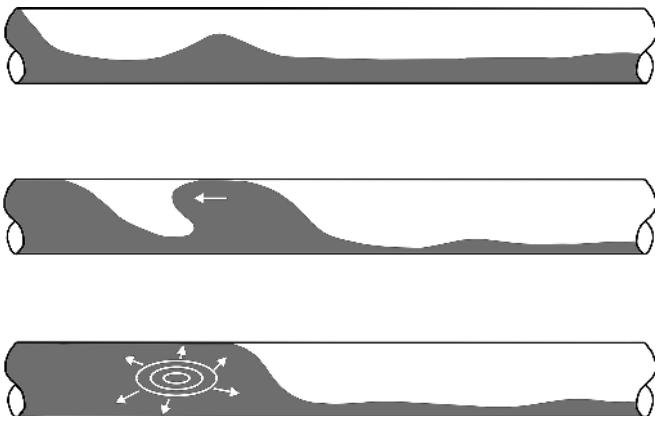

Fig. 1. Schematic representation of a sequence leading to CIWH (water: white, steam: grey)

IAC transport equation was introduced by Kocamustafaogullari and is presented in [7]. As the IAC transport equation was initially developed for vertical two-phase flow additional adjustments had to be performed for its applicability to horizontal two-phase flow, [6]. ATHLET treats the transition from stratified to slug flow in a horizontal two-phase flow based on the local void fraction and a critical gas threshold velocity according to Kelvin-Helmholtz theory presented in [8]. Validation simulations employing the adapted IAC transport equation have been performed on the basis of 50 experiments presented in [7] and the results have been reported in [9]. The detailed overview over the implementation of the IAC transport equation into the system analysis code ATHLET was presented in detail in [6].

For the calculation of the HTC, a newly developed model by [10] based on Higbie's Surface Renewal Theory (SRT) has already been implemented into the system analysis code ATHLET. The concept of surface renewal was initially developed, by Higbie [11] for the calculation of gas absorption into liquids, but it can be extended to heat transfer based on the analogy between heat and mass transfer.

Phenomenologically the SRT is based on the concept of small liquid volumes which are considered to reach the two-phase interface where they interact with the gaseous phase before being removed and transported back into the liquid bulk by turbulent eddies. A continuous scalar exchange is directly controlled by the exposure time of the small liquid volumes at the interface. Mass transfer occurring at the interface is governed by molecular diffusion during the contact time between the small liquid volumes and the interface. In an analogy with convective mass and heat transfer one can say that the SRT accounts for convective transport of small liquid volumes carrying mass and energy by turbulent eddies which can break through the laminar sub-layer of the liquid in contact with the interface and replace the already saturated small liquid volumes at the interface with fresh, sub-cooled liquid volumes from the fluid bulk. The assumption that the liquid offers the only resistance to the heat transfer influenced by its thermo-physical properties holds as long as the gaseous phase remains at saturation, which is applicable in the analyzed case of DCC. Through this mechanism heat and mass transfer are controlled by the contact time at the surface represented by the interface. Physically, the contact time reflects the time spent by eddies interacting with the two-phase interface. It therefore, controls the amount of energy and mass that can be transferred across the surface.

Figure 2 shows a schematic representation of a horizontal slug flow, with the corresponding eddies responsible for the heat removal from the interface towards the liquid bulk. It is obvious, that in different regions of the flow, different eddy scale sizes exist. Therefore considering only one eddy length scale for the calculation of the HTC for all turbulent intensities would not be appropriate. Due to this reason ATHLET employs a hybrid SRT based heat transfer model accounting for two different eddy length scales.

Hughes and Duffey [12] proposed a SRT based model which considers only microscopic eddies for the calculation of the HTC. This model relies on the concept that the smallest scales in a turbulent flow, i.e. the Kolmogorov micro-scales, are responsible for the heat removal. An assumption which holds for very small eddies, according to the hypothesis of isotropic turbulence. Shen [13] developed a model considering that larger, more energetic eddies transport the energy away from the liquid surface. An approach also used in the k-epsilon turbulence model, often employed in multi-dimensional computational fluid dynamics simulations. The final form of the model accounting for macroscopic eddies is reported in [14].

ATHLET's hybrid HTC model accounts for both microscopic and macroscopic eddies for the removal of heat from the saturated two-phase interface towards the liquid bulk, based on a turbulent Reynolds number criterion. The hybrid model is based on the assumption that the energy is carried predominantly by small eddies when the turbulent Reynolds exceeds a threshold value, in the present work 2500, while below this value bigger eddies are used for the calculation of the HTC, [15].

4 Description of the experimental facilities

4.1 The LEI test facility used for detailed investigation of the DCC phenomenon

A schematic representation of the experimental facility built at LEI for the detailed investigation on the DCC phenomenon is depicted in Fig. 3. The facility consists of the following

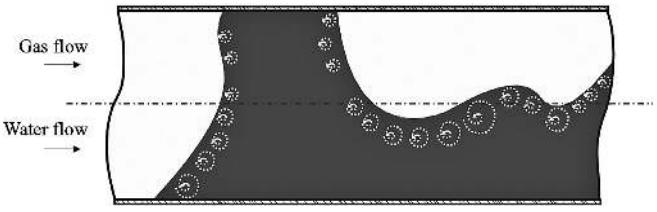

Fig. 2. Schematic representation of a slug flow with the corresponding eddies responsible for the heat removal from the interface towards the liquid bulk, (water: black, steam: white

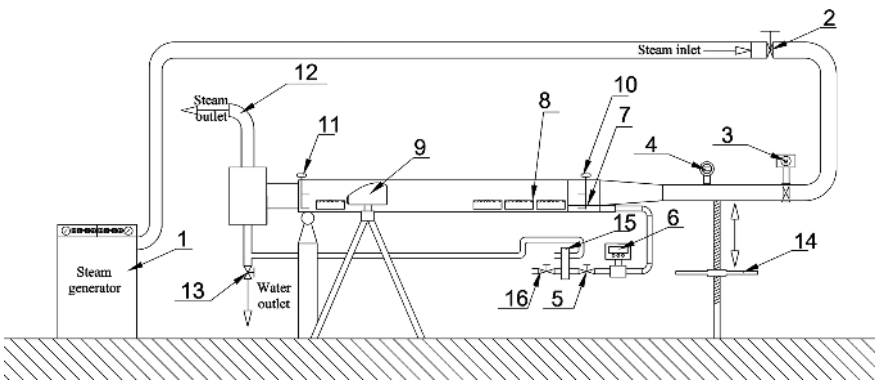

Fig. 3. Schematic representation of the LEI experimental facility. 1 – steam generator, 2 – steam inlet valve, 3 – steam flow control valve, 4 – steam flow rate meter, 5 – water flow control valve, 6 – water flow rate meter, 7 – "knife" for water surface smoothing, 8 – observation windows, 9 – infrared camera SC-5000, 10, 11 – K type thermocouples, 12 – steam outlet, 13 – water outlet, 14 – regulator of channel inclination, 15 – heat exchanger, 16 – water flow control valve

main components: a steam generator, the water supply system, water and steam inlet valves and a rectangular channel serving as the test section. The installed instrumentation includes: flow meters, thermocouples, and an infrared camera for optical investigations of the DCC phenomenon. The maximum thermal output of the steam generator is 96 kW, providing slightly overheated steam to the test section with a temperature of approx. 110 °C at atmospheric pressure in order to compensate for the limited condensation on the channel walls. Sub-cooled water is supplied to the test section with an inlet temperature of approx. 25 °C, through a heat exchanger. The water inlet velocity can be varied between 0.014 m/s and 0.056 m/s, while the steam velocity could be varied from 6 m/s to 10 m/s resulting in a ratio of steam inlet velocity to water inlet velocity of 100 to 700.

The rectangular channel of the test section with its inner dimensions of $1\,030\ \text{mm} \times 100\ \text{mm} \times 20\ \text{mm}$ $(\text{L} \times \text{H} \times \text{W})$ is made of 10 mm thick stainless steel thermally insulated with wool. At the inlet of the rectangular channel a blade was installed to separate the steam and water areas and to ensure a smooth two-phase interface, while the two-phase flow was stabilized by including a "honey comb" structure in the cross-section of the inlet. At the outlet of the test section a stair is mounted which helps to stabilize the water level in the channel at the value of 25 ± 1 mm. The inlet and outlet water temperatures were measured using K-type thermocouples. One side-wall of the rectangular channel was designed to contain 4 observations windows, at the axial locations corresponding to 166 mm, 312 mm, 458 mm and 935 mm from the inlet in order to offer the possibility of visual flow observation and the use of an infrared camera to acquire high resolution temperature measurement data. These observation windows are made of a metal ceramic material and are labelled later in the figures based on the relative axial distance to channel height (x/H): 9.4; 14.8; 20.4 and 39.2 respectively.

The infrared camera measures the water temperature with a spatial resolution of 81 measurement points/1 [mm^2] and a maximum depth of 30 μm from the side wall. For the reconstruction of the temperature profiles, measurement data belonging to a time interval of 30 s recorded with a frequency of 50 Hz was used, resulting in a total frame number of 1 500 per experiment post-processed with the ALTAIR program.

The LEI experimental facility was used for several measurement campaigns. Four representative experiments, exemplifying the impact of the phase specific inlet velocity on the vertical water temperature profile, will be presented in the following chapter.

4.2 Description of the PMK-2 experimental facility

Water hammer experiments have been performed at the integral thermal-hydraulic PMK-2 facility which models parts of a WWER-440 nuclear power plant, after the initial facility was extended by a main steam line model. A schematic drawing of the water hammer test section of the PMK-2 facility, the main steam line is presented in Fig. 4.

The PMK-2 experimental facility, built at the KFKI Institute in Hungary, has complex set up and flow characteristics. The facility was used for a total of 33 water hammer experiments during the WAHALoads project, [16]. During all 33 experiments sub-cooled water at various mass flow rates were provided to the test-section through a 73 mm inner-diameter pipe, initially filled with saturated steam. Relevant acquired measurement data included the recordings from the four local void-temperature sensors, the three pressure transducers and the void fraction distribution from the wire mesh sensor.

5 Experimental results at the LEI test facility

As output of the experiments water temperature profiles are measured at the LEI test facility. The first presented experiment has the lowest inlet phase velocities out of the four tests analyzed in this paper. The water inlet velocity corresponds to 0.014 m/s while the steam inlet velocity corresponds to 6 m/s. In the stream-wise illustration of the flow development, Fig. 5, it can be noticed that the water temperature is well stratified at the relative locations x/H = 9.4 and x/H = 14.8. At the next downstream location, corresponding to x/H = 20.4, a perturbation of the different temperature layers based

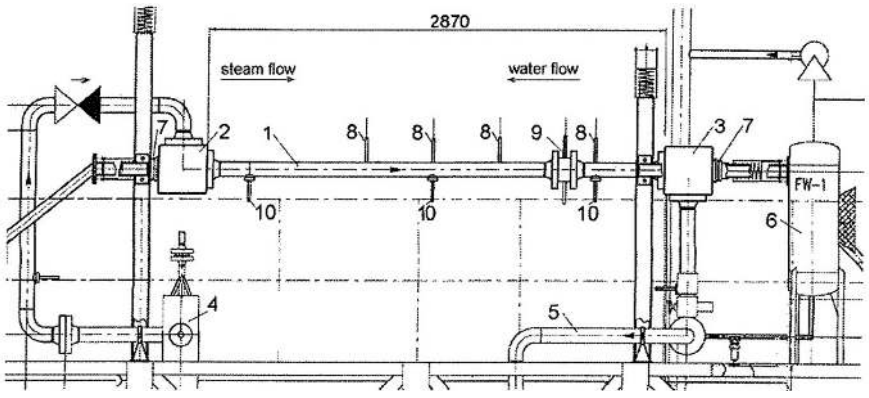

Fig. 4. Schematic representation of the PMK-2 experimental facility. 1 – horizontal test rig, 2 – inlet head, 3 – outlet head, 4 – steam generator head, 5 – connecting pipe to condenser, 6 – feed-water tank, 7 – displacement cell, 8 – local void probe with integrated thermocouple, 9 – wire mesh sensor, 10 – pressure transduce [4]

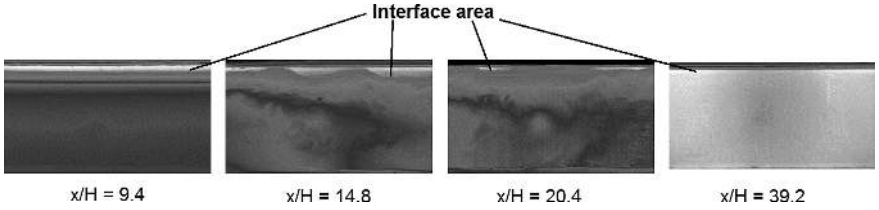

Fig. 5. Water side thermal pictures, for the water inlet velocity of 0.014 m/s and steam inlet velocity of 6 m/s. Water inlet temperature is 298 K (25 °C). Water flow direction is from left to right (dark corresponds to the lowest local temperature; Bright color corresponds to 373 K)

on an increased water turbulence can be observed, which according to the classical turbulence theory based on the Reynolds number should not arise as the water flows laminar (Re ~ 600) from the inlet of the rectangular channel (x/H = 0) to the location corresponding to x/H = 20.4. At the last location corresponding to x/H = 39.2, the liquid temperature is homogenized and even some liquid vortexes are observed below the smooth two-phase interface.

In the case of the experiment with the steam inlet velocity of 10 m/s and water inlet velocity of 0.014 m/s, depicted in Fig. 6, a relatively large water velocity gradient can be observed near the two-phase interface as the velocity close to this region is higher comparing with that of the bulk. Due to influence of the water vortexes, a flow reversal can be observed in the lower regions of the channel at the relative locations x/H = 14.8 and x/H = 20.4. The hotter water from the interface travels to the bottom of the test section while cold one flows towards the two-phase interface. Therefore, the water temperature in the central region of the cross-section is lower than near the bottom and the water surface. At the last measurement location, corresponding to x/H = 39.2 a very well homogenized water temperature can be observed. An approximately 60 % increased steam inlet velocity compared to the first experiment, resulted in a shift of the location of turbulence onset towards the two inlets. Additionally the water temperature stratification in the last measuring plane clearly highlights the impact of the steam inlet velocity on DCC and the water temperature stratification.

In the experiment with a water inlet velocity of 0.056 m/s corresponding to an increase by a factor of four compared to the value of the previously presented experiment and a steam inlet velocity of 6 m/s, the measured temperature shows a very well defined stratification almost through the entire length of the test section, as can be observed in Fig. 7. Still a transition from laminar to turbulent flow occurs for the liquid phase somewhere between the measurement locations corresponding to x/H = 20.4 and x/H = 39.2. The flow required a 3–4 times longer distance to transit from a laminar to a turbulent flow regime if the water inlet velocity is increased from 0.014 m/s to 0.056 m/s while the steam inlet velocity remains constant at 6 m/s as observed if the thermal pictures presented in Fig. 5 are compared to those of Fig. 7. This two experiments highlight the low impact of the liquid inlet velocity on the development of vortexes as the temperature measurement reflect a stable and well defined stratification almost through the entire test section.

If after the four time increase of the liquid phase from 0.014 m/s to 0.056 m/s also the velocity of the gaseous phase is increased from 6 m/s to 10 m/s, it can be noticed that the smooth temperature layers are disturbed relative fast, based on the measurement presented in Fig. 8. Figure 8 illustrates that large vortexes appear very close to the inlet sections, x/H = 14.8, and will not decay through downwards in the test section. The full excitation of water turbulence starts in the region between the measurement point corresponding to x/H 14.8 and x/H 39.2.

To summarize the observations made during the four experiments performed at the LEI facility it can be said that even for phase inlet velocities corresponding to low Reynolds numbers and thus to a laminar flow within the test section at a certain location the liquid flow becomes turbulent, as an eddy-like structure is visible in the liquid. The turbulence onset is highly dependent on the steam and water inlet velocities. The impact of an increased steam inlet velocity is clearly stronger than that of an increased water inlet velocity. This observed effect was called "turbulence excitation" and can be described as follows. Due to DCC of steam within the test section a heat-up of the liquid side occurs, resulting in a water level increase due to condensation. The interfacial shear due to the large difference in inlet velocities between steam and water is the most important parameter to mechanically disturb the structure of the two-phase interface, while the gravitational force, the viscous force and the surface tension tend to stabilize it. The influence of the surface tension could not be assessed experimentally, as the system pressure is not variable and because the water temperature near the two-phase

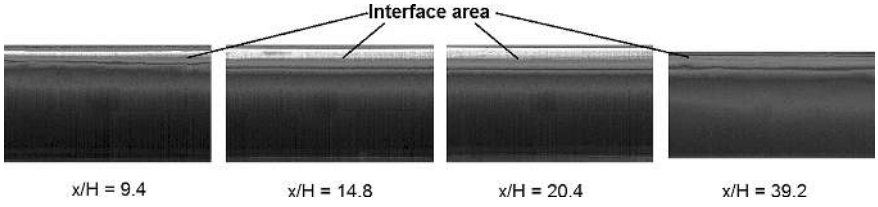

Fig. 6. Water side thermal pictures, for the water inlet velocity of 0.014 m/s and steam inlet velocity of 10 m/s. Water inlet temperature is 298 K. Water flow direction is from left to right (dark corresponds to the lowest local temperature; Bright color corresponds to 373 K)

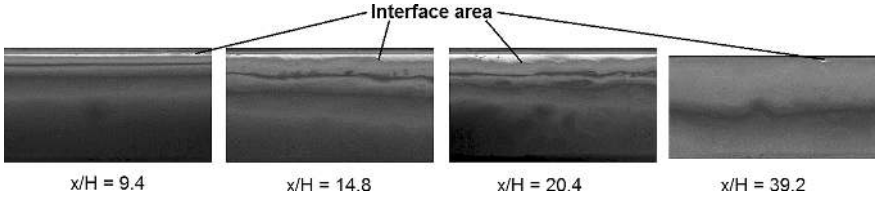

Fig. 7. Water side thermal pictures, for the water inlet velocity of 0.056 m/s and steam inlet velocity of 6 m/s. Water inlet temperature is 25 °C. Water flow direction is from left to right (dark corresponds to the lowest local temperature; Bright color corresponds to 373 K)

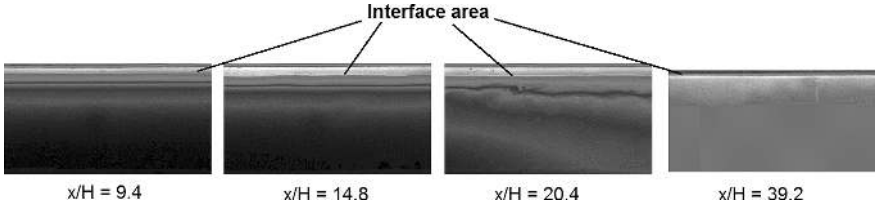

Fig. 8. Water side thermal pictures, for the water inlet velocity of 0.056 m/s and steam inlet velocity of 10 m/s. Water inlet temperature is 298 K. Water flow direction is from left to right (dark corresponds to the lowest local temperature; Bright color corresponds to 373 K)

interface is fixed and close to saturation, resulting in an impossibility to vary it. The viscosity of the liquid phase on the other hand, has a high gradient in the channel cross-section, varying with a factor of 3.5 below the two-phase interface and within the bulk. The water viscosity plays a key role in processes such as turbulence, condensation intensity, and slip velocity. Starting from the inlet of the rectangular channel, water and steam interact; therefore the interface structure is influenced by the interfacial friction force which directly depends on the slip velocity. If therefore the average slip velocity is kept constant, the local water velocity near the interface can still vary considerably due to condensation. The local slip velocity decreases in the downstream direction of the test section as the steam tends to drag and accelerate the water. DCC further increases the steam velocity near the water surface thus again increasing the slip velocity. This experimentally new found effect called "Condensation-turbulence self-induction" is characterized by:

- A water temperature increase resulting in a decrease of both its viscosity and density.
- Due to the Archimedes force warmer water, with lower density, accumulates near two-phase interface while below a thin film of temperature stratification is formed.
- The water temperature further increases within these layers decreasing the viscosity further and again enhancing the turbulence. Under the two-phase interfaces the phenomenon of so-called "turbulence excitation" occurs.
- The turbulence caused by the interfacial shear moves towards the liquid bulk as the surface is renewed with "fresh" water, increasing the condensations potential.
- The steam velocity is increased at the interface due to larger steam condensation and so is the slip velocity, creating additionally to the temperature gradient within the liquid layers also a large velocity gradient. This velocity gradient potentially creates a local flow reversal in the liquid layers.

Growing eddies destabilize the interfacial surface and "snatch" within deeper water layers.

6 Verification and validation of ATHLET for CIWH against measurements of PMK-2

All 33 experiments of the PMK-2 CIWH series have been simulated with ATHLET 3.1A using two different one-dimensional computational grid resolutions: in the simulation later labeled L/D = 2 a length of the control volume to pipe diameter ratio of two was chosen for the nodalization, while L/D = 1 was twice as fine as the previous one. The computational grid with the lowest resolution consists of 32 control volumes.

Considering the stochastic nature of CIWH the calculation of the exact timing and amplitude of the pressure surge are difficult to use as a successful validation criteria. The stochastic effect of slug appearance and interface morphology is strongly related to the two-phase flow turbulence, the apparent randomness of the slug forming location is influenced by the Kelvin-Helmholtz instability growth and has a great impact on the water hammer magnitude. A set of identical experiments are required to be performed to show the reproducibility of the phenomena observed. A repetition of an experiment at the PMK-2 facility, with identical initial conditions, underlines the nature of CIWH: during the first try a 10 MPa pressure peak was recorded, while in the second experiment a 21 MPa peak was measured, [17]. The information about the time and location of the CIWH, in these repeated experiments, is not available, still highlighting the non-reproducibility behavior of this phenomenon.

A sensitivity study on the magnitude of the pressure surge, based on characteristic parameters such as the turbulence, the flow regime, the condensation potential and the density differences between the two phases for all 33 CIWH experiments carried out at the PMK-2 integral facility was performed based on two different nodalization resolutions and the results are presented in Fig. 9 to Fig. 12. The non-dimensional numbers Reynolds (Re), Froude (Fr), Jakob (Ja) and Atwood (At) were used to account for this effects. This study was carried out in order to better understand the sensitivity of the magnitude of CIWH and event occurrence on the individual characteristic parameters and the grid resolution.

The color convention in the presented plots is the following: the experimental data is represented using a red circle, the ATHLET simulation data obtained employing the coarse grid (L/D = 2) is represented with a blue triangle, the simulation results using the higher resolution grid (L/D = 1) are represented with a green triangle. As the analyzed experiments are fully transient, the evaluation of the non-dimensional numbers has been performed for the initial quasi-steady-state conditions and used as abscissae for the plots. The ordinate

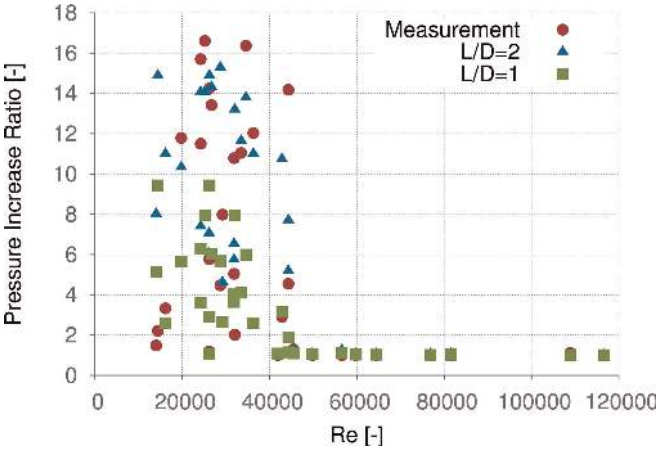

Fig. 9. Pressure Increase Ratio as a function of the Re number. The color convention in the presented plots is the following: the experimental data is represented using a circle, the ATHLET simulation data obtained employing the coarse grid (L/D = 2) is represented with a triangle, the simulation results using the higher resolution grid (L/D = 1) are represented with a square

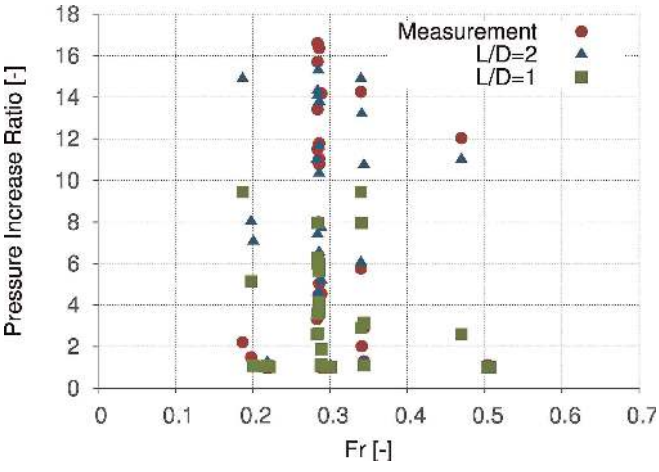

Fig. 10. Pressure Increase Ratio as a function of the Fr number

was always the pressure increase ratio, i. e. the ratio of the maximum recorded pressure to the initial system pressure for each experiment. The pressure increase ratio serves hereby as an indicator of the CIWH magnitude.

At first the influence of turbulence characterized by the liquid side Reynolds number is analyzed, and presented in Fig. 9. The highest pressure increase ratios are clustered around Re numbers of 20,000 and 40,000. Considering the relationship between the Reynolds and the Froude number, the given geometry and the thermo-physical properties of water for the given system conditions, the maximum pressure increase rates correspond to $Fr \approx 0.3$. This can also be noticed from the plot presenting the maximum amplitude of CIWH as a function of the Fr number, Fig. 10. It can be remarked that an optimum value of turbulence and a specific flow pattern have to coexist in order to generate CIWH events. An increased Reynolds number alone would lead to a Froude number larger than unity, consequently reflecting a flow pattern with a low IAC which would not lead to a CIWH event.

As expected the condensation potential, expressed by means of the Jakob number, influences directly both the probability of occurrence of the CIWH and its pressure increase ratio, Fig. 11. This is due to the direct link between the pressure surge and the condensation rate, which has been observed to be able to change, autonomously, the flow pattern from horizontal stratified to slug flow.

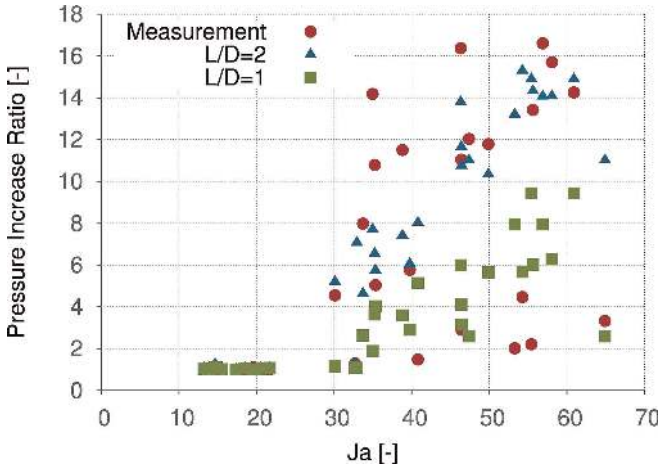

Fig. 11. Pressure Increase Ratio as a function of the Ja number

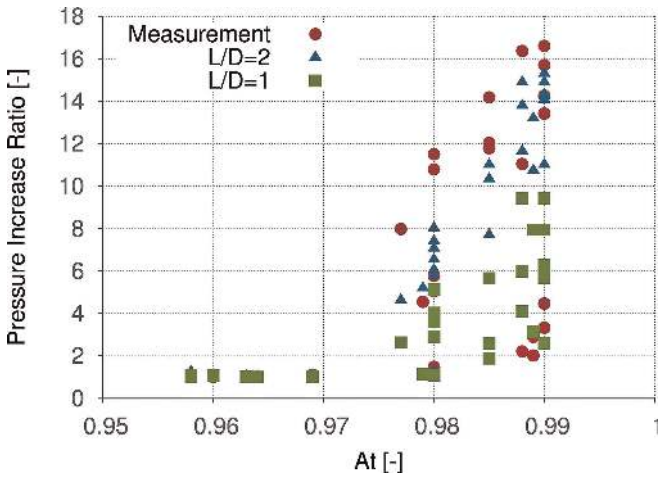

Fig. 12. Pressure Increase Ratio as a function of the At number

The high density ratio between the two phases expressed by means of the Atwood number is an important factor influencing the magnitude of the pressure surge, as water has to fill the space of the condensed steam pocket. For low system pressure the Atwood number tends to unity; resulting in very high density ratios and correspondingly to possible high pressure amplitudes of the resulting CIWH events, depicted in Fig. 12. The fact that for lower At numbers, simultaneously both the number of CIWH events and their magnitude abruptly drop to zero, underlines the conclusion that facilities operating at low system pressures are more prone to CIWH incidents than facilities operating at high system pressure, as higher system pressure the densities of the phases converge to a similar order of magnitude. It can be highlighted that the plots, both created based on the measured data and on the simulation results with the modified system analysis code, exhibit a maximum pressure increase rate around $Re \approx 20.0000$ with a clear influence from Jacob number. For experiments corresponding to smaller Re values, almost no CIWH events are recorded or simulated. The sensitivity study analyzing the nodalization resolution highlighted an important impact of this parameter on the pressure surge magnitude. In general it can be stated that the coarser nodalization enhances the CIWH potential, due to a higher sub-cooling of the liquid in control volumes containing both phases. This is not necessary an improvement of the system codes simulation results towards a best-estimate statement but rather towards conservatism. A computational grid sensitivity study is therefore advised when the CIWH phenomenon is analyzed.

7 Conclusions and outlook

Experiments focusing on the in-depth analysis of the DCC phenomena haven been investigated at the Lithuanian Energy Institute based on a stratified co-current two-phase flow within a narrow rectangular channel by measuring the water temperature profiles with a high resolution infrared camera. The results of the experiments show that the steepness of water thermal gradient near the two-phase interface can be explained by Archimedes principle. A consequence of this effect is that water layers with lower density and viscosity come in contact with the faster moving steam triggering an excitation of turbulence in water bulk. Due to this excitation of turbulence in the water bulk region an increase in steam condensation can be observed. Additionally the experiments noted that the increase in inlet velocity for each phase had a different impact on the flow development. The increase of only the steam velocity by maintaining a constant water velocity shifts the location of turbulence onset closer to test section inlet, while only an increase of the inlet water velocity shifts the onset location downstream towards the test section outlet. An increase of both inlet velocities broadens the region in the test section were turbulent flow occurs, thus overlapping both individual effects.

The numerical investigations performed with ATHLET 3.1A highlighted that the simultaneous usage of the hybrid, mechanistic, HTC model together with the IAC transport equation, enhance the applicability range of the system analysis code to the field of DCC driven water hammer. This enhancement is reached without the need of any special parameter tuning, thus offering the system analysis code predictive capabilities for this phenomenon, still the results are sensitive to the computational grid resolution. The current work aims to assess the capabilities of the system analysis code ATHLET based on mechanistic models, to be able to capture

CIWH phenomena during horizontal two-phase flows involving complex dynamic interaction mechanisms and not to qualify ATHLET as a pressure surge computer code. Consequently only a qualitative validation against measurement data was performed.

ATHLET is clearly capable to correctly account the individual influences of turbulence, flow character, condensation potential and the differences in density between the two phases, for the analysis of the CIWH. Nevertheless the development of the hybrid SRT based HTC model together with the IAC transport equation for horizontal two-phase flow will be continued at the GRS alongside an extensive validation process.

Acknowledgements

The part of this work performed at the GRS was carried out on behalf of the German Federal Ministry for Economic Affairs and Energy on the basis of a decision by the German Bundestag.

(Received on 1 March 2016)

References

1 *Cahill, W. J.*: Feedwater line incident report – Indian Point Unit No. 2. Consolidated Edison Co., AEC Docket No. 50–247, 1974
2 *Almenas, K.; Pabarcius, R.; Seporaitis, M.*: Design and tests of a device for the generation of controlled condensation implosion events. Heat Transfer Engineering 27 (2006) 32–41, DOI:10.1080/01457630500458047
3 *Valincius, M.; Seporaitis, M.; Kaliatka, A.; Pabarcius, R.; Gasiunas, S.; Laurinavicius, D.*: The concept and RELAP5 model of thermal-hydraulic system employing a rapid condensation for coolant circulation. Heat Transfer Engineering 35 (2014) 327–335, DOI:10.1080/01457632.2013.810965
4 *Kulisch, H.; Dirndorfer, S.; Dörfler, M.; Malcherek, A.*: Condensation-induced water hammer – overview and own experiments. Proc. of the 14th Intl. Topical Meeting on Nuclear Reactor Thermal-Hydraulics, 2011
5 *Urban, C.; Schlüter, M.*: Investigations on the stochastic nature of condensation induced water hammer. Int. J. of Multiphase Flow 67 (2014) 1–9, DOI:10.1016/j.ijmultiphaseflow.2014.08.001
6 *Austregesilo, H.; Trambauer, K.*: Modelling of the Interfacial Area Concentration in the System Code ATHLET. Proc. of the 11th Intl. Topical Meeting on Nuclear Reactor Thermal-Hydraulics, 2005
7 *Kocamustafaogullari, G.; Ishii, M.*: Foundations of the interfacial area transport equation and its closure relations. Intl. J. of Heat Mass Trans 38 (1995) 481–493, DOI:10.1016/0017-9310(94)00183-V
8 *Taitel, Y.; Dukler, A. E.*: A Model for Predicting Flow Regime Transitions in Horizontal and Near Horizontal Gas-Liquid Flow. AIChE Journal 22 (1976) 47–55, DOI:10.1002/aic.690220105
9 *Trambauer, K.; Austregesilo, H.; Bals, Ch.; Cester, F.; Deitenbeck, H.; Klein-Heßling, W.; Lerchl, G.; Müller, Ch.; Papukchiev, A.; Schubert, J. D.*: Continued development of the computer code system ATHLET/ATHLET-CD. Gesellschaft für Anlagen und Reaktorsicherheit (GRS) mbH, Reactor Safety Research-Project 2009 No.: RS 1162.
10 *Ceuca, C. S.; Macián-Juan, R.*: Development of a 1 D hybrid HTC model using CFD simulations for the analysis of direct contact condensation as the driving force for water hammers. Kerntechnik 78 (2013) 25–30, DOI:10.3139/124.110307
11 *Higbie, R.*: The rate of absorption of a pure gas into a still liquids during a short time of exposure. Transactions of AIChE 31 (1935) 365–389
12 *Hughes, E. D.; Duffey, R. B.*: Direct contact condensation and momentum transfer in turbulent separated flows. Intl. J. of Multiphase Flow 17 (1991) 599–619, DOI:10.1016/0301-9322(91)90027-Z
13 *Shen, L.; Triantafyllou, G. S.; Yue, K. P. D.*: Turbulent diffusion near a free surface. J. of Fluid Mechanics 407 (2000) 145–166, DOI:10.1017/S0022112099007466
14 *Egorov, Y.; Boucker, M.; Martin, A.; Pigny, S.; Scheuerer, M.; Willemsen, S.*: Validation of CFD codes with PTS-relevant test cases 5th EURATOM FRAMEWORK PROGRAMME 1998–2002. 2004, Technical report
15 *Kolev, N. I.*: Multiphase Flow Dynamics II. 2007, Berlin: Springer-Verlag, p. 605–631, DOI:10.1007/3-540-69833-7
16 *Prasser, H. M.; Ézsöl, G.; Baranyai, G.; Sühnel, T.*: Spontaneous waterhammers in a stream line in case of cold water ingress. Multiphase Sci. Technol. 20 (2008) 265–289, DOI:10.1615/MultScienTechn.v20.i3-4.30
17 *Barna, I. F.; Imre, A. R.; Baranyai, G.; Ézsöl, G.*: Experimental and theoretical study of steam condensation induced water hammer phenomena. Nuclear Engineering and Design, 240 (2010) 146–150, DOI:10.1016/j.nucengdes.2009.09.027

The authors of this contribution

Dr.-Ing. *Sabin Cristian Ceuca* (corresponding author)
E-mail: sabin.ceuca@grs.de
Gesellschaft für Anlagen- und Reaktorsicherheit (GRS) gGmbH
Boltzmannstr. 14, 85748 Garching, Germany
M. Sc. *Darius Laurinavičius*
Lithuanian Energy Institute
Breslaujos Str. 3, 44403 Kaunas, Lithuania

Bibliography
DOI 10.3139/124.110729
KERNTECHNIK
81 (2016) 5; page 504–511

ISSN 0932-3902

Books · Bücher

History, Development and Future of TRIGA Research Reactors. Published by the International Atomic Energy Agency, 2016, IAEA Technical Report Series No. 482, ISBN 978-92-0-102016-1, 113 pp., 45.00 EUR.

Due to its particular fuel design and resulting enhanced inherent safety features, TRIGA reactors (Training, Research, Isotopes, General Atomics) constitute a "class of their own" among the large variety of research reactors built world-wide. This publication summarizes in a single document the information on the past and present of TRIGA research reactors and presents an outlook in view of potential issues to be solved by TRIGA operating organizations in the near future. It covers the historical development and basic TRIGA characteristics, followed by utilization, fuel conversion and ageing management of TRIGA research reactors. It continues with issues and challenges, introduction to the global TRIGA research reactor network and concludes with future perspectives. The publication is complemented with a CD-ROM to illustrate the historical developments of TRIGA research reactors through individual facility examples and experiences.